Overexpression of the SETD2 WW domain inhibits the phosphor-IWS1/SETD2 interaction and the oncogenic AKT/IWS1 RNA splicing program.

Georgios I. Laliotis[a,b,c,1,3], Evangelia Chavdoula[a,b], Vollter Anastas[a,b,d], Satishkumar Singh[e], Adam D. Kenney[f], Samir Acharya[a,b,2], Jacob S. Yount[f], Lalit Sehgal[b,e] and Philip N. Tsichlis[a,b,3]

[a]The Ohio State University, Department of Cancer Biology and Genetics, Columbus, OH, 43210, [b]The Ohio State University Comprehensive Cancer Center-Arthur G. James Cancer Hospital and Richard J. Solove Research Institute, Columbus, OH, 43210, [c]University of Crete, School of Medicine, Heraklion Crete, 71500, Greece, [d]Tufts Graduate School of Biomedical Sciences, Program in Genetics, Boston, MA, 02111, USA, [e]College of Medicine, Department of Hematology, The Ohio State University, Columbus, OH 43210, [f]Department of Microbial Infection and Immunity, The Ohio State University, Columbus, OH, 43210

Running Title: SETD2 WW domain inhibits the IWS1 RNA splicing program

Present address :

[1]Department of Oncology, Sidney Kimmel Comprehensive Cancer Center, Johns Hopkins School of Medicine, Baltimore, MD, 21231

[2]Nationswide Children's Hospital, Columbus, OH, 43205

[3]Correspondence should be addressed to: Philip N. Tsichlis (Lead contact) (Philip.tsichlis@osumc.edu) or Georgios I. Laliotis (glaliot1@jhmi.edu)

Abstract

Our earlier studies had shown that AKT phosphorylates IWS1, and that following phosphorylation, IWS1 recruits the histone methyltransferase SETD2 to an SPT6/IWS1/ALY complex, which assembles on the Ser2-phosphorylated CTD of RNA Pol II. Recruited SETD2 methylates histone H3 at K36, during transcriptional elongation of target genes, and this regulates multiple steps in RNA metabolism. By regulating the RNA splicing of *U2AF2,* it controls cell proliferation. Importantly, pathway activity correlates with histological grade, clinical stage, and metastatic potential of lung adenocarcinomas, especially those with *EGFR* mutations. By regulating nucleocytoplasmic mRNA transport of intronless genes, including those encoding type I IFNs, it regulates sensitivity to viral infection. Here, we show that SETD2 interacts with IWS1 via its WW domain, that the interaction is IWS1 phosphorylation-dependent, and that WW domain overexpression blocks the interaction and inhibits the pathway and its biological outcomes. We conclude that blocking the phosphor-IWS1/SETD2 interaction is feasible and has significant therapeutic potential in human cancer.

Significance

IWS1 phosphorylation by AKT, primarily AKT3, promotes tumor cell proliferation and correlates positively with the histological grade, clinical stage, and metastatic potential of lung adenocarcinomas, especially those with *EGFR* mutations. Therefore, targeting the phosphor-IWS1 pathway may benefit patients with these tumors. Inhibiting AKT3 should block this pathway. However, we do not currently have clinical grade AKT3-specific inhibitors, and even if we did, inhibition of AKT3 would have off target effects. Here, we show that SETD2 binds phosphor-IWS1 via its 33 aa-long WW domain and that overexpression of this domain blocks the phosphor-IWS1/SETD2 interaction, inhibiting the pathway and tumor cell proliferation in culture and in animals. Therefore, blocking the phospho-IWS1/SETD2 interaction is feasible and has significant therapeutic potential in human cancer.

56 **Introduction**

57 Earlier studies had shown that IWS1 interacts with, and recruits SETD2 to an
58 SPT6/IWS1/ALY complex, which assembles on the Ser2-phosphorylated CTD of RNA Pol II
59 (Yoh et al., 2007[1]) and that the SETD2 recruitment depends on the phosphorylation of IWS1
60 at Ser720/Thr721 by AKT (Sanidas et al., 2014[2], Laliotis et al., 2021[3]). The binding of SETD2
61 to the SPT6/phospho-IWS1 complex results in trimethylation of Histone H3 at K36 during
62 transcriptional elongation (Yoh et al., 2007[1]). Whereas the phosphorylation of IWS1 regulates
63 the recruitment of SETD2, it does not affect the interaction between IWS1 and the other
64 components of the SPT6/IWS1/ALY/SETD2 complex (Sanidas et al., 2014[2]).

65 The recruitment of SETD2 to the SPT6/IWS1/ALY complex and the trimethylation of
66 Histone H3 in the body of genes targeted by this complex, has profound effects on the biology
67 of NCI-H522 and other NSCLC cell lines. Our earlier studies had shown that it regulates the
68 alternative RNA splicing of *FGFR2*, favoring the *FGFR2* IIIc splice variant (Sanidas et al.,
69 2014[2]), which is primarily expressed in mesenchymal cells (Luco et al., 2010[4]), and which, in
70 cancer cells, promotes epithelial to mesenchymal transition and cell migration, invasiveness
71 and metastasis (Thiery et al., 2006[5]). RNA-Seq studies, comparing the gene expression
72 profiles of NCI-H522 cells transduced with shControl, or shIWS1 constructs, and shIWS1-
73 transduced NCI-H522 cells rescued with wild type IWS1 (WT-R) or with the phosphorylation
74 site IWS1 mutant (MT-R), revealed genome wide IWS1 and IWS1 phosphorylation-dependent
75 changes in gene expression and RNA processing (Laliotis et al., 2021[3]). Importantly, many of
76 the genes whose expression and/or RNA processing were deregulated in shIWS1 and
77 shIWS1/MT-R cells, were genes encoding proteins involved in epigenetic regulation and RNA
78 processing.

79 One of the genes undergoing IWS1 phosphorylation-dependent alternative RNA
80 splicing, is the *U2AF2* gene, which encodes the core RNA splicing factor U2AF65. The
81 predominant *U2AF2* mRNA in empty vector (shControl) and shIWS1/WT-R cells contain exon
82 2, which is absent from the predominant *U2AF2* mRNA in shIWS1 and shIWS1/MT-R cells.
83 Exon 2 encodes part of the N-terminal RS domain of U2AF65, which interacts with several

84 proteins involved in the regulation of RNA processing. One of these proteins is Prp19, a
85 member of an RNA splicing complex with ubiquitin ligase activity (Prp19C), which is composed
86 of four core and three accessory polypeptides and plays a critical role in spliceosomal
87 activation (Chanarat et al., 2013[6]). Prp19 is recruited to the phosphorylated CTD of RNA Pol
88 II, via its interaction with U2AF65 (David et al., 2011[7]). In vitro RNA splicing experiments have
89 shown that the U2AF65/Prp19 binding promotes the splicing of exons located downstream of
90 weak polypyrimidine tracts (David et al., 2011[7]). Our more recent studies provided evidence
91 that by regulating *U2AF2* RNA splicing, IWS1 phosphorylation promotes the expression of
92 *CDCA5*, which encodes Sororin, a member of the Cohesin complex, and that by regulating
93 this pathway, IWS1 phosphorylation plays a critical role in cell cycle regulation and cell
94 proliferation (Laliotis et al., 2021[3]). In addition, IWS1 phosphorylation-dependent RNA splicing
95 promotes the nucleocytoplasmic transport of the mRNAs of intronless genes that harbor
96 Cytoplasmic Accumulation Region Elements (CAR-E). This set of genes includes the genes
97 encoding type I interferons, whose expression is impaired when the pathway is disrupted
98 (Laliotis et al., 2021[8]). Most importantly, the IWS1 phosphorylation pathway correlates
99 positively with the grade, clinical stage and metastatic potential of lung adenocarcinomas,
100 especially those with activating mutations or amplification of the gene encoding *EGFR*. As a
101 result, patients with *EGFR* mutant lung adenocarcinomas exhibit higher relapse rates after
102 treatment, and shortened survival (Laliotis et al., 2021[3]).

103 Based on the preceding observations, we hypothesized that targeting this pathway
104 may have significant therapeutic implications in lung adenocarcinomas with *EGFR* mutations,
105 and perhaps in other types of human cancer. Inhibiting AKT3, the AKT isoform primarily
106 responsible for the activation of the pathway, should block this pathway. However, we do not
107 currently have clinical grade AKT3 specific inhibitors and even if we did, inhibition of AKT3
108 would have multiple off target effects, because AKT3 does not only regulate this pathway.
109 Based on these considerations, we proceeded to investigate whether inhibiting the interaction
110 between IWS1 and SETD2 is feasible, and what would be the biological consequences of
111 blocking this interaction. The IWS1 domain interacting with SETD2 had been mapped earlier

112 to a sequence which extends from amino acid 522 to amino acid 698 and includes part of the
113 TFIID homologous IWS1 domain (Yoh et al., 2008[9]). As a first step therefore, we mapped the
114 SETD2 domain interacting with phosphorylated IWS1, and we showed that it is limited to a 40
115 amino acid peptide, which includes the 33 amino acid WW domain of SETD2 (2391-2422aa).
116 Following mapping of the interacting domains, we showed that the WW domain of SETD2
117 interacts preferentially with the phosphorylated form of IWS1, and that when overexpressed,
118 it blocks the interaction of the two proteins and inhibits the pathway activated via this
119 interaction. More important, overexpression of the WW domain of SETD2, inhibits tumor cell
120 proliferation in culture and tumor growth in xenograft models in animals, suggesting that
121 blocking the interaction of SETD2 with phosphorylated IWS1 is feasible and has significant
122 therapeutic potential in human cancer.

123 **Results**

124 **The interaction between SETD2 and phosphorylated IWS1 is mediated by the WW**
125 **domain of SETD2.**

126 Our first task prior to developing strategies to block the AKT phosphorylation-dependent
127 interaction between IWS1 and SETD2, was to map the SETD2 domain interacting with
128 phosphorylated IWS1. To this end, we generated a series of Hemagglutinin (HA)-tagged
129 deletion mutants of SETD2 (**Fig. 1A**), which we expressed via transient transfection in the
130 NCI-H522 and NCI-H1299 lung adenocarcinoma cell lines and we used co-
131 immunoprecipitation to determine their interaction with endogenous IWS1. Based on these
132 experiments we mapped the IWS1-interacting SETD2 domain to a 40 amino acid peptide,
133 which includes the 33 amino acid WW domain (aa 2391-2422) and surrounding sequences
134 (**Fig. 1B and 1C**).

135 **The WW domain of SETD2 binds selectively IWS1 phosphorylated at Ser720/Thr721 and**
136 **disrupts the interaction of IWS1 with SETD2**

137 Our earlier studies had shown that SETD2 is recruited to an SPT6/IWS1/ALY-REF
138 complex, following phosphorylation of IWS1 at Ser720/Thr721, by AKT1 or AKT3. This
139 observation raised the question whether the binding of the WW peptide of SETD2 to IWS1
140 also depends on IWS1 phosphorylation. To address this question, we expressed Flag-tagged
141 constructs of wild type IWS1 or its phosphorylation site mutant in the lung adenocarcinoma
142 cell lines NCI-H522, NCI-H1299, A549 and NCI-H1975. Following this, we transduced the
143 cells with a V5-tagged construct of the SETD2 WW domain. Probing V5 (WW domain)
144 immunoprecipitates with the Flag-tag (IWS1) antibody and Flag-tag immunoprecipitates with
145 the V5 tag antibody, revealed that the WW domain of SETD2 indeed interacts with IWS1, but
146 the interaction is significantly more robust with wild type than with mutant IWS1 (**Fig. 2A**).
147 These observations strongly suggest that the interaction of the WW domain of SETD2 with
148 IWS1 continues to be IWS1 phosphorylation-dependent and therefore physiologically
149 relevant.

150 Following the demonstration that the WW domain of SETD2 interacts selectively with
151 phosphorylated IWS1, we examined whether overexpression of this domain inhibits the
152 IWS1/SETD2 interaction. First, we addressed the interaction of exogenous Flag-tagged wild
153 type IWS1 with HA-SETD2, and following this, the interaction of the endogenous proteins. Co-
154 immunoprecipitation experiments confirmed that the overexpression of the WW domain of
155 SETD2 inhibits the interaction of both the exogenous and the endogenous proteins (**Fig. 2B**
156 **and 2C**).

157 **Overexpression of the SETD2 WW domain inhibits the IWS1 phosphorylation-**
158 **dependent RNA splicing program.**

159 The observation that overexpression of the SETD2 WW domain blocks the interaction
160 between phosphorylated IWS1 and SETD2, suggested that it would also interfere with IWS1

161 phosphorylation-dependent alternative RNA splicing. Our earlier studies identified several
162 IWS1 phosphorylation-dependent RNA splicing targets, including *U2AF2* (exon 2), *SLC12A2*
163 (exon 21), *IFT88* (exon 8), *C1qTNF6* (exon 3), *STXBP1* (exon 18) and *FGFR2* (exon 8)
164 (Laliotis et al., 2021[3] , Sanidas et al., 2014[2]). Transduction of the four lung adenocarcinoma
165 cell lines used for the experiments in figure 2 with a pLx304-based lentiviral construct of the
166 SETD2 WW domain revealed that overexpression of this domain reproduces the alternative
167 RNA splicing pattern of the IWS1 knockdown in all six genes (**Fig. 3A, 3D**). To determine
168 whether the WW domain-induced changes in alternative RNA splicing are due to inhibition of
169 the IWS1 phosphorylation pathway, we examined the binding of SETD2 and the abundance
170 of H3K36me3 marks, in selected regions of the *U2AF2* and *FGFR2* genes in NCI-H522 and
171 NCI-H1299 cells transduced with the pLx304-WW domain construct. The *U2AF2* and *FGFR2*
172 Transcription Start Sites (TSS) and *GAPDH* Exon 3 (E3) were used as controls. This was
173 addressed with Chromatin ImmunoCleavage (ChIC) experiments, which showed that the WW
174 domain of SETD2 dramatically inhibits the binding of SETD2 and the abundance of histone
175 H3K36me3 marks (**Fig. 3C, 3D**). These experiments provided proof of principle for the
176 feasibility of blocking the IWS1/SETD2 interaction and for the ability of the block to inhibit the
177 IWS1 phosphorylation-dependent regulation of RNA processing. Based on our earlier findings
178 on the biology elicited by the IWS1 phosphorylation pathway, these data also suggested the
179 blocking this pathway by overexpressing the SETD2 WW peptide should have a major impact
180 on the pathobiology of lung adenocarcinomas and perhaps other types of human cancer.

181 **Overexpression of the WW domain of SETD2 inhibits pathways regulated by the**
182 **alternative RNA splicing of *U2AF2.***

183 The exon 2-defficient splice variant of *U2AF2,* which is expressed in shIWS1 and
184 shIWS1/MT-R cells, is defective in the processing of the *CDCA5* pre-mRNA (Laliotis et al.,
185 2021[3]). This results in the downregulation of the *CDCA5* protein product, Sororin. The latter is
186 involved in the regulation of ERK phosphorylation, the expression of CDK1 and Cyclin B1, and
187 the regulation of the G2/M phase of the cell cycle (Laliotis et al., 2021[3]). Cells expressing the

188 exon 2-deficient *U2AF2* are also defective in the nucleocytoplasmic transport of the mRNAs
189 of a set of intronless genes that harbor CAR-Elements, including *JUN*, *HSPB3* (encoding
190 HSP27), *IFNA1* and *IFNB1* (encoding IFNα1 and IFNβ1 respectively) (Laliotis et al., 2021[8]).
191 We therefore asked whether, by promoting the skipping of *U2AF2* exon 2, the overexpression
192 of the WW domain of SETD2 also inhibits the phosphorylation of ERK and the expression of
193 CDK1 and Cyclin B1, as well as the expression and ERK-dependent phosphorylation of JUN,
194 and the expression of HSP27 and type I IFNs. The results confirmed the prediction by showing
195 that the WW domain of SETD2 reproduces the IWS1 knockdown ERK phosphorylation, cell
196 cycle and RNA transport phenotypes (**Fig. 4A, 4B**). Type I IFNs in this experiment were
197 induced by Sendai virus infection (Laliotis et al., 2021[8]) (**Fig. 4B**).

198 Collectively, these results show that overexpression of the SETD2 WW domain inhibits
199 the endogenous IWS1/SETD2 interaction (**Fig. 2**), the binding of SETD2 and the abundance
200 of H3K36me3 marks in select regions of target genes, the IWS1 dependent-alternative RNA
201 splicing of the targets of the IWS1 phosphorylation pathway (**Fig. 3)**, and signaling pathways
202 controlled by these targets (**Fig. 4**).

203 **Overexpression of the SETD2 WW domain inhibits cell cycle progression and**
204 **proliferation of lung adenocarcinoma cell lines, and anchorage-independent growth of**
205 **Human Bronchial Epithelia Cells (HBECs) transduced with IWS1-S720D/T721E**
206 **(IWS1/DE).**

207 Our earlier studies had shown that the IWS1 phosphorylation pathway is cell cycle-
208 regulated, and that its inhibition profoundly affects the proliferation of lung adenocarcinoma
209 cell lines. Given that the overexpression of the SETD2 WW domain inhibits this pathway, we
210 examined its effects on the proliferation of four lung adenocarcinoma cell lines (NCI-H522,
211 NCI-H1299, A549 and NCI-H1975) in culture. The same cells transduced with shIWS1 were
212 used as controls. The results showed that the proliferation of 2D cultures of all four cell lines
213 was significantly impaired when the cells were transduced with a lentiviral construct of the WW
214 domain (**Fig. 5A**). Flow-cytometric analysis of log phase cultures of NCI-H522, NCI-H1299,

215 A549 and NCI-H1975 cells transduced with shControl, shIWS1 or pLx304-SETD2/WW
216 constructs and stained with Propidium Iodide (PI), confirmed that the overexpression of the
217 WW domain of SETD2 results in partial G2/M arrest, as expected (**Fig. 5B**).

218 To determine whether the partial G2/M arrest and the inhibition of cell proliferation by
219 the overexpressed WW domain of SETD2 are because of the overexpression on the
220 alternative RNA splicing of *U2AF2*, we examined the ability of the RS domain-containing
221 U2AF65α and the RS domain-deficient U2AF65β to rescue the hypo-proliferative phenotype
222 induced by the overexpression of the WW domain. The results confirmed that whereas
223 U2AF65α rescues the phenotype, U2AF65β does not (**Fig. 5C**, **Fig. S1A, S1B**). However, the
224 rescue was only partial, suggesting that overexpression of the WW domain of SETD2 may
225 inhibit cell proliferation by targeting the alternative RNA splicing of *U2AF2*, in addition to other
226 targets, which have not been identified to-date.

227 In parallel experiments, we overexpressed the SETD2 WW domain in human bronchial
228 epithelial cells immortalized with the telomerase catalytic subunit hTERT, (hTERT-HBEC) and
229 transformed with the constitutively active phosphomimetic mutant IWS1-DE. hTERT-HBECs
230 transduced with the empty vector pLx304, were used as controls. The soft agar colony growth
231 data in these cells showed that the WW domain inhibits anchorage-independent cell growth
232 (**Fig. 5D**). These data were consistent with the proliferation data in the lung adenocarcinoma
233 cell lines, described in the preceding paragraph.

234

235 **Overexpression of the SETD2 WW domain blocks the IWS1 phosphorylation pathway**
236 **and inhibits the growth of NCI-H1299 mouse xenografts.**

237 The data in the preceding paragraphs confirmed that the inhibition of cell proliferation and
238 transformation by the SETD2 WW domain is due, at least in part, to the inhibition of the pIWS1
239 /*U2AF2* /*CDCA5* pathway, which based on our earlier observations, is strongly pro-oncogenic
240 (Laliotis et al., 2021[3]). This raised the question whether the SETD2 WW domain peptide
241 inhibits the growth of lung adenocarcinoma mouse xenografts. The experiment addressing
242 this question was done, using two groups of NSG (NOD.Cg-*Prkdc*^{scid} *Il2rg*^{tm1Wjl}/SzJ) mice (**Fig.**

243 **6A**). Group 1 was inoculated subcutaneously in the flanks with NCI-H1299 cells transduced
244 with a lentiviral shIWS1 construct, or with the empty lentiviral vector (shControl) (7 mice each,
245 14 mice total). Group 2 was inoculated similarly with NCI-H1299 cells transduced with the
246 same shIWS1 lentiviral vector used in group 1, or with a SETD2 WW domain construct in the
247 lentiviral vector pLx304 (also 7 mice each, 14 mice total) (**Fig. 6A**). The animals were
248 monitored for tumor growth, and they were sacrificed 4 weeks later. The results confirmed that
249 both the loss of IWS1 and the overexpression of the SETD2 WW domain, significantly reduce
250 tumor growth. Notably, the inhibition of tumor growth in mice inoculated with NCI-H1299 cells
251 engineered to overexpress the SETD2 WW domain was more robust than the inhibition of
252 tumor growth in mice inoculated with shIWS1-transduced cells (**Fig. 6B**). This observation
253 supports the hypothesis that the SETD2 WW domain may inhibit cell proliferation by targeting
254 not only the alternative RNA splicing of *U2AF2*, but also other cell proliferation-promoting
255 targets.

256 Based on the preceding data and the role of the IWS1 phosphorylation pathway in
257 tumor cell proliferation in culture and in animals (Sanidas et al., 2014[2], Laliotis et al., 2021[3]
258 and this report), we hypothesized that the WW domain of SETD2 would inhibit the interaction
259 of IWS1 with SETD2 in mouse xenografts, and by inhibiting the interaction, would also inhibit
260 xenograft growth. This was confirmed with co-immunoprecipitation experiments, which
261 showed that overexpression of the SETD2 WW domain indeed inhibits the interaction between
262 IWS1 and SETD2 (**Fig. 6C**). The expression of the SETD2 WW domain and the abundance
263 of IWS1 and phosphor-IWS1 in these tumors, were confirmed by western blotting (**Fig. 6D**).
264 Using RT-PCR we also addressed the alternative RNA splicing of confirmed targets of the
265 IWS1 phosphorylation pathway. The results showed that in mouse xenografts, like in cultured
266 cells, overexpression of the SETD2 WW domain dramatically inhibits the IWS1
267 phosphorylation-dependent alternative RNA splicing pathway (**Fig. 6D**). Next, we probed
268 western blots of tumor cell lysates with antibodies to Sororin, phosphor-ERK (Y202/T204),
269 CDK1, Cyclin B1 and PCNA, all of which are regulated by the IWS1 phosphorylation-
270 dependent alternative RNA splicing of *U2AF2* (Laliotis et al., 2021[3]). The results confirmed

271 that the WW domain also inhibits the phosphorylation of ERK and the expression of these
272 regulators of the cell cycle (**Fig. 6D**). We conclude that overexpression of the SETD2 WW
273 domain inhibits tumor growth, by inhibiting the IWS1/U2AF2/CDCA5 pathway and cell cycle
274 progression.

275 IWS1 phosphorylation controls the alternative RNA splicing of *FGFR2*, favoring the
276 *FGFR2* mRNA splice variant IIIc. This variant is expressed primarily in mesenchymal cells,
277 and it has been shown to promote epithelial to mesenchymal transition (EMT) in cancer cells.
278 We therefore questioned whether the overexpression of the SETD2 WW domain inhibits the
279 expression of EMT markers in the developing tumors. Immunohistochemistry experiments,
280 addressing the expression of ZEB1, TWIST and Vimentin confirmed this prediction (**Fig. 6D**).

281 Representative examples of the histology of the tumors derived from shControl,
282 shIWS1 and pLx304-SETD2 WW domain-transduced NCI-H1299 cells (**Fig. 6E)**. The same
283 figure also shows representative examples of immunohistochemistry experiments addressing
284 the expression of the Ki-67 proliferation marker, ZEB1, TWIST and Vimentin in the same
285 tumors. Whereas the histology of the tumors derived from the control cells was similar to the
286 histology of the tumors derived from cells engineered to express the WW domain of SETD2,
287 the results of the Ki-67 ZEB1, TWIST and Vimentin immunohistochemistry experiments
288 revealed that overexpression of the WW domain of SETD2, resulted in the downregulation of
289 all these markers (**Fig. 6F**). Quantification of the abundance of Ki-67 ZEB1, TWIST and
290 Vimentin in all the same tumors confirmed the results (**Fig. 6E**) and was consistent with the
291 western blot data (**Fig. 6D)**.

292 Overall, the data in this report support the model in figure 7. According to this model,
293 the SETD2 WW domain binds phosphorylated IWS1, and by doing so it antagonizes the
294 interaction of phosphor-IWS1 with SETD2 and the recruitment of SETD2 to the RNA
295 elongation complex assembling on the Ser2-phosphorylated CTD of RNA Pol II. Blocking the
296 recruitment of SETD2 to the complex prevents histone H3K36 trimethylation in the body of
297 target genes during transcriptional elongation. Given the importance of H3K36me3 marks in
298 RNA elongation and RNA processing, the loss of these marks results in major shifts in RNA

299 splicing and other RNA processing events. This alters the IWS1 phosphorylation-dependent
300 H3K36me3 distribution and subsequent oncogenic AKT/IWS1 RNA splicing program, leading
301 to inhibition of tumor growth Changes in the RNA splicing of *U2AF2* inhibit tumor cell
302 proliferation, while changes in the RNA splicing of *FGFR2* inhibit both tumor cell proliferation
303 and the expression of EMT markers (**Fig. 7**).

304 In addition to showing that blocking the interaction of phosphor-IWS1 with SETD2 is
305 feasible and has profound effects on the biology of tumor cells, the data in this report also
306 provide information for the design of a strategy to screen for small molecules to inhibit the
307 interaction. Such molecules hold promise for the therapeutic targeting of the AKT/phosphor-
308 IWS1 pathway in lung adenocarcinomas and potentially other types of human cancer.

309 **Discussion**

310 Although AKT is known to play a major role in most types of human cancer, its
311 therapeutic targeting has been only minimally successful to-date. This may be due to several
312 reasons. First, there are three AKT isoforms which functionally overlap, but also have non-
313 overlapping, and in some cases opposing functions (Song et al., 2019[10], Wang et al., 2018[11]).
314 This suggests that using inhibitors that target all AKT isoforms, which is the case for most of
315 the inhibitors available to-date, may have suboptimal results. Another reason is that AKT has
316 wide reaching effects in cell signaling, both in normal and in cancer cells (Manning et al.,
317 2017[12]), and its inhibition may result in significant toxicity. One way to address these limitations
318 is to identify and selectively target AKT-regulated signaling pathways with critical roles in
319 human cancer. One such pathway is the IWS1 phosphorylation pathway, which is activated
320 by AKT in a cell cycle-dependent manner and epigenetically regulates transcription, RNA
321 metabolism and perhaps other epigenetically regulated processes, and has a major role in
322 human lung adenocarcinomas and most likely in other forms of human cancer (Sanidas et al,
323 2014[2], Laliotis et al, 2021[3]). In this report we present our initial data on a strategy aiming to
324 selectively target this pathway.

325 The knockdown of IWS1 in human lung adenocarcinoma cell lines, and its rescue with
326 the S720A/T721A IWS1 mutant, which cannot be phosphorylated by AKT, result in significant

327 inhibition of cell proliferation in culture and tumor growth in xenograft models in
328 immunocompromised mice. Our recent studies provided a mechanistic explanation for this
329 observation, by showing that IWS1 is induced and undergoes phosphorylation by AKT during
330 the transition from the G1 to the S phase of the cell cycle, and that following phosphorylation,
331 it regulates the alternative RNA splicing of multiple genes, one of which is *U2AF2,* the gene
332 encoding the core RNA splicing factor U2AF65. The predominant *U2AF2* mRNA in cells with
333 low abundance of phosphorylated IWS1 lacks exon 2, which encodes the RS domain of
334 U2AF65, a domain that is required for the interaction of U2AF65 with additional RNA splicing
335 regulators, including Prp19. The loss of the Prp19-interacting domain impairs the recruitment
336 of the Prp19 complex (Prp19C) to the spliceosome, resulting in defects in the processing and
337 nucleocytoplasmic transport of the mRNAs of multiple genes. One of these genes is *CDCA5,*
338 which encodes Sororin, a member of the Cohesin complex (Zhang et al., 2012[13]). The IWS1-
339 regulated Sororin is phosphorylated by ERK and the phosphorylated Sororin enhances ERK
340 phosphorylation by an unknown mechanism. This Sororin/ERK feedback loop promotes
341 progression through the G2/M phase of the cell cycle and cell proliferation (Laliotis et al,
342 2021[3]).

343 As indicated above, the IWS1 phosphorylation-dependent alternative RNA splicing of
344 *U2AF2* also regulates the nucleocytoplasmic transport of the mRNAs of a set of intronless
345 genes, which harbor Cytoplasmic Accumulation Region Elements (CAR-E). The absence of
346 IWS1 phosphorylation, therefore, lowers the nuclear export of these mRNAs and the
347 abundance of the proteins they encode. Genes, whose regulation by this mechanism has been
348 confirmed, include *JUN*, *HSPB3* (encoding Hsp27), *IFNA1* and *IFNB1* (encoding IFNα1 and
349 IFNβ1 respectively). The abundance of these proteins may affect cell proliferation and survival
350 in response to external signals, in addition to regulating the sensitivity to viral infection (Laliotis
351 et al., 2021[8]).

352 *FGFR2* is also known to undergo alternative RNA splicing and our earlier studies had
353 shown that its RNA splicing is also regulated by IWS1 phosphorylation. The latter promotes
354 the skipping of exon 8, giving rise to the IIIc mRNA transcript, which is observed in

355 mesenchymal cells and is associated with Epithelial to Mesenchymal Transition (EMT). The
356 loss of IWS1 phosphorylation on the other hand, promotes the inclusion of exon 8, giving rise
357 to the IIIb mRNA transcript of *FGFR2*, which is observed in epithelial cells. By regulating the
358 alternative RNA splicing of *FGFR2*, the IWS1 phosphorylation pathway also promotes EMT,
359 cell migration and tumor cell invasiveness. By regulating these pathways, IWS1
360 phosphorylation contributes to cell transformation in culture and to tumor growth in animals.
361 More important, this pathway is active in human lung adenocarcinomas, especially those with
362 EGFR mutations, and the activity of the pathway correlates with tumor stage, histologic grade,
363 metastasis, relapse after treatment, and poor prognosis.

364 The first step in the activation of the IWS1 pathway is the recruitment of SETD2 to an
365 SPT6/IWS1/ALY-REF complex, which assembles on the Ser2-phosphorylated CTD of RNA
366 Pol II. The signal for the recruitment of SETD2 is the phosphorylation of IWS1 by AKT. The
367 work presented in this report focuses on the question whether we can block the interaction
368 between phosphorylated IWS1 and SETD2 and whether blocking this interaction will result in
369 the reversal of the known phenotypic effects of the pathway in cancer cells. Using deletion
370 mutants of SETD2 and co-immunoprecipitation assays in HEK293 cells we mapped the IWS1-
371 interacting domain of SETD2 to its WW domain, a short, 33 amino-acid peptide. The SETD2
372 WW domain is preceded by a proline-rich stretch and the same is observed in the WW
373 domains of other proteins, including Huntingtin. NMR studies of the Huntingtin WW domain
374 have shown that it interacts with the proline-rich stretch, and that the interaction between the
375 two domains results in a closed conformation (Gao et al., 2014[14]). If the interaction between
376 these domains is conserved in SETD2 as expected, it may have an auto-inhibitory role. In this
377 case, the binding to phosphorylated IWS1, may allosterically activate SETD2. This finding is
378 significant because it suggests that the binding of SETD2 to the CTD complex does not only
379 link SETD2 to the machinery that will allow it to methylate chromatin during transcriptional
380 elongation, but that it may also activate it.

381 The WW domain is defined by the presence of two tryptophan (W) residues 20-23 aa
382 apart (Vargas et al., 2019[15], Jäger et al., 2006[16]). WW domains bind proline-rich protein

383 regions, including proline-rich phosphor-tyrosine and phosphor-serine-threonine sites (Ingham
384 et al., 2005[17], Sudol et al., 2010[18], Salah et al., 2012[19]). By binding to their targets, they
385 transduce signals along signaling cascades, and they regulate the cytoskeleton and cell
386 polarity (Lin et al., 2019[20], Ilsley et al., 2002[21]). Changes in the interaction between WW
387 domains and their targets have been linked to genetic disorders, such as the Liddle syndrome
388 (Pucheta-Martinez et a., 2016[22], Chang et al., 2019[23], Sudol et al., 2012[24]) muscular dystrophy,
389 Huntington's chorea, Alzheimer's disease (Kunkle et al., 2019[25]) and cancer (Salah et al.,
390 2011[26], Lee et al., 2012[27], Hung et al., 2020[28]). Based on the motifs they bind, five classes of
391 WW domains have been identified to-date. The most common is Class I, which recognizes
392 the sequence (L/P)Pp(Y/poY), where L and P stand for Leucine and Proline respectively, po
393 identifies a phosphorylated residue and lower case letters represent favored, but not
394 conserved residues. Class II recognizes PPLPp motifs, class III recognizes PR or PXR-rich
395 motifs and class V recognizes motifs characterized by uninterrupted stretches of prolines.
396 Particularly interesting is class IV, which recognizes motifs containing a phosphorylated Serine
397 or Threonine, followed by Proline (poS/poT)P (Salah et al., 2012[19]). The IWS1 domain
398 interacting with SETD2 extends from amino acid 548 to amino acid 698 (Yoh et al., 2008[9]).
399 Analysis of this sequence identified a potential class IV phosphor-SP motif (Lu P.J. et al
400 1999[29]), which overlaps with a class II-like PLPX motif and a PXR sequence, which can be
401 part of a class III motif. Importantly, the extended region around these motifs contains several
402 Proline, Arginine and Lysine residues, which may contribute to the interaction of IWS1 with
403 the SETD2 WW domain. (**Fig. S2**). However, the role of these motifs in the phosphor-
404 IWS1/SETD2 interaction remains to be confirmed.

405 Data in figure 5 showed that the proliferation defect induced by the overexpression of
406 the WW domain of SETD2 in lung adenocarcinoma cell lines is rescued, but only partially, by
407 the RS domain containing U2AF65 isoform, U2AF65α. Moreover, the data in figure 6, showed
408 that the growth inhibition of tumor xenografts engineered to overexpress the WW domain of
409 SETD2, is more robust than the growth inhibition induced by the IWS1 knockdown. These
410 data combined, suggest that the overexpression of the WW domain of SETD2 may inhibit cell

411 proliferation by targeting the alternative RNA splicing of *U2AF2*, in addition to other targets
412 that have not been identified to-date. p53, which interacts with the WW domain of SETD2 via
413 its N-terminal transactivation domain (aa 1-45) is unlikely to be one of these targets, because
414 its interaction with SETD2 stimulates the expression of many of the anti-proliferative and pro-
415 apoptotic genes it regulates (Xie et al, 2008[30]). Therefore, blocking its interaction with SETD2
416 should inhibit the expression of these genes. In addition, p53 should not be relevant to some
417 of the cell lines we used in this study, including NCI-H1299, which is p53-null, and perhaps
418 NCI-H522 and NCI-H1975, which harbor point mutations in p53. Another protein known to
419 interact with the WW domain of SETD2 is Huntingtin (Gao et al., 2014[14], Seervai et al., 2020[31]).
420 SETD2 bound to Huntingtin and the actin-binding adaptor HIP1R, trimethylates Actin at K68.
421 ActK68me3 localizes to the F-actin cytoskeleton and regulates actin
422 polymerization/depolymerization. Blocking actin methylation, which is expected to occur in
423 cells overexpressing the WW domain of SETD2, inhibits cell migration (Seervai et al., 2020[31])
424 and perhaps cell survival (Cisbani et al., 2012[32]).
425 In summary, data presented in this report, provide robust evidence that selective
426 inhibition of the IWS1 phosphorylation pathway has a strong therapeutic potential. In addition,
427 they show that blocking the interaction between phosphorylated IWS1 and SETD2 is feasible,
428 and it can effectively inhibit the pathway. Finally, they provide a roadmap for strategies that
429 can be employed to identify small molecule inhibitors of the pathway.
430

431 **Materials and Methods**

432 **Cells and culture conditions, growth factors and inhibitors**

433 Cells, shRNAs, retroviral and lentiviral constructs and experimental protocols, including cell
434 culture conditions, retroviral and lentiviral packaging, and cellular transduction with retroviral
435 and lentiviral constructs, are described in detail in the Supplemental Information.

436 **Cell Proliferation, cell transformation and Cell cycle analysis**

437 Proliferation of cells growing under normal culture conditions was monitored using the Incucyte
438 S3 Live-Cell Imaging and Analysis System (Essen Biosciences, Ann Arbor, MI). Captured data
439 were analyzed using the native analysis software. The cell transformation assay was
440 performed using the Cell Transformation Assay Kit-Colorimetric (Abcam Cat No. ab235698),
441 as previously described (Laliotis et al., 2021[3]). The cell cycle distribution of exponentially
442 growing cells was monitored by flowcytometry of ethanol-fixed, propidium iodide-stained cell
443 cultures. For details see Supplemental Information.

444 **Sendai Virus propagation and titration and utilization for the induction of type I IFNs.**

445 The Sendai-GFP (SeV-GFP) propagation, titration and infection was performed as previously
446 described (Yount et al., 2006[33], Laliotis et al., 2021[8]). For details, see Supplemental
447 Information.
448

449 **RT-PCR and qRT-PCR**

450 RT-PCR and qRT-PCR were carried out as previously described (Laliotis et al., 2021[3]). Total
451 RNA was isolated using the PureLink RNA Kit (Invitrogen, Cat. No 12183018A). Isolated RNA
452 was analyzed by real-time RT-PCR for the expression of the indicated mRNAs. The mRNA
453 levels were normalized based on the levels of *GAPDH* (internal control). The primer sets and
454 procedural details are described in the Supplemental Information.

455 **Immunoblotting and Protein Immunoprecipitation**

456 Cells were lysed with RIPA buffer and cell lysates were electrophoresed in SDS-PAGE and
457 analyzed by immunoblotting. Protein immunoprecipitation was carried out, as described
458 previously (Laliotis et al., 2021[3]), with minor modifications. Images were acquired and
459 analyzed, using the Li-Cor Fc Odyssey Imaging System (LI-COR Biosciences, Lincoln, NE).

460 For the lists of antibodies used for immunoprecipitation and western blotting and for procedural
461 details, see Supplemental Information.

462 **Chromatin Immuno-Cleavage (ChIC)**

463 The binding of SETD2 and the abundance of histone H3K36me3 on target genes, were
464 addressed by chromatin Immuno-cleavage (Skene et al., 2018[34,] Laliotis et al., 2021[3]). For
465 details, see Supplemental Information.

466 **Tumor xenografts**

467 NOD.*Cg-Prkdc*^{scid} *Il2rg*^{tm1Wjl}/SzJ (NSG) mice were injected subcutaneously with 2x10^{6} NCI-
468 H1299 and they were monitored for 4 weeks. Tumor metrics, protein and RNA extraction,
469 tumor immunohistochemistry and signal quantification were performed as previously
470 described (Laliotis et al., 2021[3]). For more details, see the Supplemental Information. All
471 mouse experiments were reviewed and approved by the Institutional Animal Care and Use
472 Committee (IACUC) of the Ohio State University.

473 **Data availability**

474 All the raw data underlying figures 1-6 (uncropped gel images, qPCR, flowcytometry, plate
475 reader, proliferation data and microscope images have been deposited in the Mendeley
476 Dataset and they are publicly available (Laliotis et al., 2021[35]). *P* values are also included in
477 the Mendeley dataset.

478 **Acknowledgments**

479 The authors wish to thank all the members of the Tsichlis Lab for helpful discussions. We are
480 grateful to Dr Michael Freitas for helpful discussions and Dr Joal Beane for reviewing the
481 manuscript prior to submission. This work was supported by the NIH grant R01 CA186729 to
482 P.N.T., the NIH grant R01 CA198117 to P.N.T and V.C, by start-up funds from the OSUCCC
483 to P.N.T. and from the National Centre for Advancing Translational Sciences grant

KL2TR002734 to L.S. G.I.L was supported by the Pelotonia Post-Doctoral fellowship from OSUCCC.

Author Contributions

G.I.L. Conceptualization, overall experimental design. Performed experiments, analysed the data, prepared the figures and wrote the manuscript. **E.C.** Designed and performed the mouse xenografts, protein and RNA extraction of mouse tumours, performed the mouse xenografts staining studies and picture acquisition and edited the manuscript **V.A.** Designed, performed, analysed the proliferation experiments and edited the manuscript **S.S.** Assisted in FACS experiments **A.D.K.** Designed, optimized and performed the infection with Sendai virus and edited the manuscript **A.K.K.** Performed RT-PCR experiments and assisted in cloning. **K.A.N** Performed RT-PCR experiments and assisted and assisted in cloning. **S.A.** Assisted in the design for SETD2 deletion mutants and edited the manuscript **J.S.Y** Advised on the viral strain infection and edited the manuscript **L.S.** Advised on the design of experiments and edited the manuscript. **P.N.T.** Conceptualization, overall experimental design, project supervision, manuscript writing and editing.

Competing Interests

The authors declare no competing interests.

Corresponding authors

Correspondence to : Philip N. Tsichlis (lead contact) and Georgios I. Laliotis

References

1. Yoh, S.M., Cho, H., Pickle, L., Evans, R.M. and Jones, K.A., 2007. The Spt6 SH2 domain binds Ser2-P RNAPII to direct Iws1-dependent mRNA splicing and export. *Genes & development*, *21*(2), pp.160-174.

508 2. Sanidas, I., Polytarchou, C., Hatziapostolou, M., Ezell, S.A., Kottakis, F., Hu, L., Guo,
509 A., Xie, J., Comb, M.J., Iliopoulos, D. and Tsichlis, P.N., 2014. Phosphoproteomics
510 screen reveals akt isoform-specific signals linking RNA processing to lung cancer.
511 *Molecular cell*, *53*(4), pp.577-590.
512 3. Laliotis, G.I., Chavdoula, E., Paraskevopoulou, M.D. *et al.* AKT3-mediated IWS1
513 phosphorylation promotes the proliferation of EGFR-mutant lung adenocarcinomas
514 through cell cycle-regulated *U2AF2* RNA splicing. *Nat Commun* **12,** 4624 (2021).
515 https://doi.org/10.1038/s41467-021-24795-1
516 4. Luco, R.F., Pan, Q., Tominaga, K., Blencowe, B.J., Pereira-Smith, O.M. and Misteli,
517 T., 2010. Regulation of alternative splicing by histone
518 modifications. *Science*, *327*(5968), pp.996-1000.
519 5. Thiery, J.P. and Sleeman, J.P., 2006. Complex networks orchestrate epithelial–
520 mesenchymal transitions. *Nature reviews Molecular cell biology*, *7*(2), pp.131-142.
521 6. Chanarat, S. and Sträßer, K., 2013. Splicing and beyond: the many faces of the Prp19
522 complex. *Biochimica et Biophysica Acta (BBA)-Molecular Cell Research*, *1833*(10),
523 pp.2126-2134.
524 7. David, C.J., Boyne, A.R., Millhouse, S.R. and Manley, J.L., 2011. The RNA polymerase
525 II C-terminal domain promotes splicing activation through recruitment of a U2AF65–
526 Prp19 complex. *Genes & development*, *25*(9), pp.972-983.
527 8. Georgios I. Laliotis, Adam D. Kenney, Evangelia Chavdoula, Arturo Orlacchio, Abdul
528 K. Kaba, Alessandro La Ferlita, Vollter Anastas, Christos Tsatsanis, Joal D. Beane,
529 Lalit Sehgal, Vincenzo Coppola, Jacob S. Yount, Philip N. Tsichlis, Phosphor-IWS1-
530 dependent *U2AF2* splicing regulates trafficking of CAR-E-positive intronless gene
531 mRNAs and sensitivity to viral infection. *Commun Biol* **4,** 1179 (2021).,
532 *http://doi.org/10.1038/s42003-021-02668-z*
533 9. Yoh, S.M., Lucas, J.S. and Jones, K.A., 2008. The Iws1: Spt6: CTD complex controls
534 cotranscriptional mRNA biosynthesis and HYPB/Setd2-mediated histone H3K36
535 methylation. *Genes & development*, *22*(24), pp.3422-3434.

536 10. Song, M., Bode, A.M., Dong, Z. and Lee, M.H., 2019. AKT as a therapeutic target for
537 cancer. *Cancer research*, *79*(6), pp.1019-1031.
538 11. Wang, J., Zhao, W., Guo, H., Fang, Y., Stockman, S.E., Bai, S., Ng, P.K.S., Li, Y., Yu,
539 Q., Lu, Y. and Jeong, K.J., 2018. AKT isoform-specific expression and activation
540 across cancer lineages. *BMC cancer*, *18*(1), pp.1-10.
541 12. Manning, B.D. and Toker, A., 2017. AKT/PKB signaling: navigating the
542 network. *Cell*, *169*(3), pp.381-405.
543 13. Zhang, N. and Pati, D., 2012. Sororin is a master regulator of sister chromatid cohesion
544 and separation. *Cell cycle*, *11*(11), pp.2073-2083.
545 14. Gao, Y.G., Yang, H., Zhao, J., Jiang, Y.J. and Hu, H.Y., 2014. Autoinhibitory structure
546 of the WW domain of HYPB/SETD2 regulates its interaction with the proline-rich region
547 of huntingtin. *Structure*, *22*(3), pp.378-386.
548 15. Vargas, R.E., Duong, V.T., Han, H., Ta, A.P., Chen, Y., Zhao, S., Yang, B., Seo, G.,
549 Chuc, K., Oh, S. and El Ali, A., 2020. Elucidation of WW domain ligand binding
550 specificities in the Hippo pathway reveals STXBP 4 as YAP inhibitor. *The EMBO*
551 *journal*, *39*(1), p.e102406.
552 16. Jäger, M., Zhang, Y., Bieschke, J., Nguyen, H., Dendle, M., Bowman, M.E., Noel, J.P.,
553 Gruebele, M. and Kelly, J.W., 2006. Structure–function–folding relationship in a WW
554 domain. *Proceedings of the National Academy of Sciences*, *103*(28), pp.10648-10653.
555 17. Ingham, R.J., Colwill, K., Howard, C., Dettwiler, S., Lim, C.S., Yu, J., Hersi, K.,
556 Raaijmakers, J., Gish, G., Mbamalu, G. and Taylor, L., 2005. WW domains provide a
557 platform for the assembly of multiprotein networks. *Molecular and cellular biology*,
558 *25*(16), pp.7092-7106.
559 18. Sudol, M., 2010. Newcomers to the WW domain–mediated network of the Hippo tumor
560 suppressor pathway. *Genes & cancer*, *1*(11), pp.1115-1118.
561 19. Salah, Z., Alian, A. and Aqeilan, R.I., 2012. WW domain-containing proteins:
562 retrospectives and the future. *Front Biosci*, *17*, pp.331-348.

563 20. Lin, Z., Yang, Z., Xie, R., Ji, Z., Guan, K. and Zhang, M., 2019. Decoding WW domain
564 tandem-mediated target recognitions in tissue growth and cell polarity. *Elife*, *8*,
565 p.e49439.
566 21. Ilsley, J.L., Sudol, M. and Winder, S.J., 2002. The WW domain: linking cell signalling
567 to the membrane cytoskeleton. *Cellular signalling*, *14*(3), pp.183-189.
568 22. Pucheta-Martinez, E., D'Amelio, N., Lelli, M., Martinez-Torrecuadrada, J.L., Sudol, M.,
569 Saladino, G. and Gervasio, F.L., 2016. Changes in the folding landscape of the WW
570 domain provide a molecular mechanism for an inherited genetic syndrome. *Scientific*
571 *reports*, *6*(1), pp.1-8.
572 23. Chang, N.S., Lin, R., Sze, C.I. and Aqeilan, R.I., 2019. WW Domain Proteins in
573 Signaling, Cancer Growth, Neural Diseases, and Metabolic Disorders. *Frontiers in*
574 *oncology*, *9*, p.719.
575 24. Sudol, M., McDonald, C.B. and Farooq, A., 2012. Molecular insights into the WW
576 domain of the Golabi-Ito-Hall syndrome protein PQBP1. *FEBS letters*, *586*(17),
577 pp.2795-2799.
578 25. Kunkle, B.W., Grenier-Boley, B., Sims, R., Bis, J.C., Damotte, V., Naj, A.C., Boland,
579 A., Vronskaya, M., Van Der Lee, S.J., Amlie-Wolf, A. and Bellenguez, C., 2019.
580 Genetic meta-analysis of diagnosed Alzheimer's disease identifies new risk loci and
581 implicates Aβ, tau, immunity and lipid processing. *Nature genetics*, *51*(3), pp.414-430.
582 26. Salah, Z. and Aqeilan, R.I., 2011. WW domain interactions regulate the Hippo tumor
583 suppressor pathway. *Cell death & disease*, *2*(6), pp.e172-e172.
584 27. Lee, H.L., Cheng, H.L., Liu, Y.F., Chou, M.C., Yang, S.F. and Chou, Y.E., 2017.
585 Functional genetic variant of WW domain-containing oxidoreductase (WWOX) gene is
586 associated with hepatocellular carcinoma risk. *PLoS One*, *12*(4), p.e0176141.
587 28. Hung, S.C., Chou, Y.E., Li, J.R., Chen, C.S., Lin, C.Y., Chang, L.W., Chiu, K.Y., Cheng,
588 C.L., Ou, Y.C., Wang, S.S. and Yang, S.F., 2020, February. Functional genetic variant
589 of ww domain containing oxidoreductase gene associated with urothelial cell

590 carcinoma clinicopathologic characteristics and long-term survival. In *Urologic*
591 *Oncology: Seminars and Original Investigations* (Vol. 38, No. 2, pp. 41-e1). Elsevier.
592 29. Lu PJ, Zhou XZ, Shen M, Lu KP. Function of WW domains as phosphoserine- or
593 phosphothreonine-binding modules. Science. 1999 Feb 26;283(5406):1325-8.
594 30. Xie, P., Tian, C., An, L., Nie, J., Lu, K., Xing, G., Zhang, L. and He, F., 2008. Histone
595 methyltransferase protein SETD2 interacts with p53 and selectively regulates its
596 downstream genes. *Cellular signalling*, *20*(9), pp.1671-1678.
597 31. Seervai, R.N., Jangid, R.K., Karki, M., Tripathi, D.N., Jung, S.Y., Kearns, S.E., Verhey,
598 K.J., Cianfrocco, M.A., Millis, B.A., Tyska, M.J. and Mason, F.M., 2020. The Huntingtin-
599 interacting protein SETD2/HYPB is an actin lysine methyltransferase. *Science*
600 *advances*, *6*(40), p.eabb7854.
601 32. Cisbani, G. and Cicchetti, F., 2012. An in vitro perspective on the molecular
602 mechanisms underlying mutant huntingtin protein toxicity. *Cell death & disease*, *3*(8),
603 pp.e382-e382.
604 33. Yount, J.S., Kraus, T.A., Horvath, C.M., Moran, T.M. and López, C.B., 2006. A novel
605 role for viral-defective interfering particles in enhancing dendritic cell maturation. *The*
606 *Journal of Immunology*, *177*(7), pp.4503-4513.
607 34. Skene, P.J., Henikoff, J.G. and Henikoff, S., 2018. Targeted in situ genome-wide
608 profiling with high efficiency for low cell numbers. *Nature protocols*, *13*(5), p.1006.
609 35. Laliotis, Georgios I; Chavdoula, Evangelia; Anastas, Vollter; Singh, Satishkumar;
610 Kenney, Adam D. ; Acharya, Samir; Yount, Jacob S.; Sehgal, Lalit; Tsichlis, Philip N.
611 (2021), "Overexpression of the SETD2 WW domain inhibits the phosphor-
612 IWS1/SETD2 interaction and the oncogenic AKT/IWS1 RNA splicing program.",
613 Mendeley Data, V1, doi: 10.17632/d5kv2dyhc4.1
614 36. Laliotis GI., Evangelia Chavdoula, Abdul Kaba, Alessandro La Ferlita, Vollter Anastas,
615 Arturo Orlacchio, Lalit Sehgal, David P. Carbone, Vincenzo Coppola and Philip N.
616 Tsichlis. '*The inhibition of IWS1 phosphorylation promotes genomic instability, the*
617 *cGAS/STING pathway activation and PD-L1 levels, through the U2AF2 alternative*

618 *RNA splicing and Sororin expression.*' October 19-20, 2020, Cancer Immunol Res
619 February 1 2021 (9) (2 Supplement) PO010; doi:10.1158/2326-6074.TUMIMM20-
620 PO010, *AACR Virtual Special Conference: Tumor Immunology and Immunotherapy*
621 37. Laliotis GI., Adam D. Kenney, Evangelia Chavdoula, Arturo Orlacchio, Vollter Anastas,
622 Alessandro La Ferlita, Abdul Kaba, Lalit Sehgal, Vincenzo Coppola, Jacob S. Yount
623 and Philip N. Tsichlis. '*Sensitivity of cancer cells to oncolytic viruses is defined by IWS1*
624 *phosphorylation dependent epigenetic regulation of U2AF2 splicing and*
625 *nucleocytoplasmic export of type I IFN transcripts*', October 19-20, 2020, Cancer
626 Immunol Res February 1 2021 (9) (2 Supplement) PO088; doi:10.1158/2326-
627 6074.TUMIMM20-PO088, *AACR Virtual Special Conference: Tumor Immunology and*
628 *Immunotherapy*;
629 38. Laliotis GI., Evangelia Chavdoula, Maria D. Paraskevopoulou, Abdul Kaba, Alessandro
630 La Ferlita, VollterAnastas, Arturo Orlacchio, Vasiliki Taraslia, Ioannis Vlachos, Marina
631 Capece, Artemis Hatzigeorgiou, Dario Palmieri, Salvatore Alaimo, Christos Tsatsanis,
632 Lalit Sehgal, David P. Carbone, Vincenzo Coppola, Philip N. Tsichlis. '*IWS1*
633 *phosphorylation promotes tumor growth and predicts poor prognosis in EGFR mutant*
634 *lung adenocarcinoma patients, through the epigenetic regulation of U2AF2 RNA*
635 *splicing*' [abstract]. October 15-16, 2020; 2020 Oct 15-16. Philadelphia (PA): AACR;
636 Cancer Res 2020;80(23 Suppl):Abstract nr PO-011., doi: 10.1158/1538-
637 7445.EPIMETAB20-PO-011, *AACR Special Virtual Conference on Epigenetics and*
638 *Metabolism*
639 39. Laliotis GI., Evangelia Chavdoula, Maria D. Paraskevopoulou, Vollter Anastas, Ioannis
640 Vlachos, Vasiliki Tarasslia, Artemis Hatzigeorgiou, Dario Palmieri, Abdul Kaba, Marina
641 Capece, Arturo Orlacchio, Lalit Sehgal, Vincenzo Coppola and Philip N. Tsichlis,
642 *'Alternative RNA splicing of U2AF2, induced by AKT3-phosphorylated IWS1, promotes*
643 *tumor growth, by activating a CDCA5-ERK positive feedback loop', Cancer Res August*
644 *15 2020 (80) (16 Supplement) 3649*; doi:10.1158/1538-7445.AM2020-3649, *American*
645 *Association of Cancer Research 2020 (AACR 2020) Virtual Conference*

646 40. Laliotis GI., Adam D. Kenney, Arturo Orlacchio, Vincenzo Coppola, Jacob S. Yount
647 and Philip N. Tsichlis, *'Sensitivity of cancer cells to oncolytic viruses is defined by IWS1*
648 *phosphorylation dependent epigenetic regulation of U2AF2 splicing and*
649 *nucleocytoplasmic export of type I IFN transcripts.'*, Cancer Res August 15 2020 (80)
650 (16 Supplement) LB-183; doi:10.1158/1538-7445.AM2020-LB-183, *American*
651 *Association of Cancer Research 2020 (AACR 2020) Virtual Conference*
652 41. Laliotis, G.I., Tsichlis, P.N., 2020. *Effective Identification of Protein-Protein Interaction*
653 *using RIME-IP*. *Protocols*. io, dx. doi. org/10.17504/protocols.io.bqx8mxrw
654 42. Laliotis, G.I., Tsichlis, P.N., *2020. Effective identification of DNA-bound protein*
655 *complexes using Chromatin Immunoprecipitation. Protocols. io,* dx.doi.
656 org/10.17504/protocols. io. Bjj6kkre.
657 43. Laliotis, G.I., Tsichlis, P.N., 2020. *Effective identification of RNA-binding proteins using*
658 *RNA Immunoprecipitation. Protocols. io,* dx. doi. org/10.17504/protocols. io. Bjpbkmin.

Figure 1

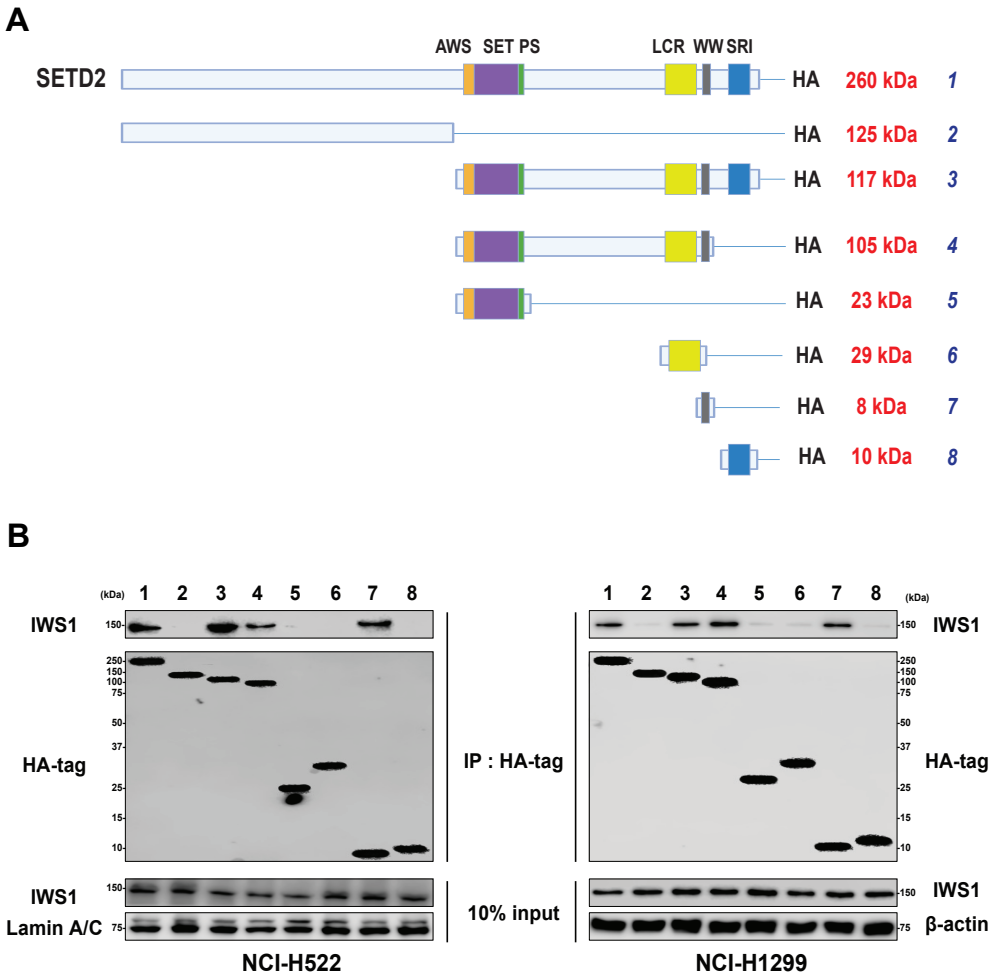
A
AWS SET PS
LCR WW SRI
SETD2
HA 260 kDa 1
HA 125 kDa 2
HA 117 kDa 3
HA 105 kDa 4
HA 23 kDa 5
HA 29 kDa 6
HA 8 kDa 7
HA 10 kDa 8
B
(kDa) 1 2 3 4 5 6 7 8
IWS1
HA-tag
IWS1
Lamin A/C
IP : HA-tag
10% input
IWS1
HA-tag
IWS1
β-actin
NCI-H522
NCI-H1299

Figure Legends

Figure 1. The interaction between SETD2 and IWS1 is mediated by the WW domain of SETD2.

- **A.** *Graphical representation of the SETD2 deletion mutants (1-8) used in this study*. AWS : Associated with SET, SET : Su(var)3–9, Enhancer-of-zeste, Trithorax, PS : post-SET, LCR : Low Charge Region, WW, SRI : Set2 Rpb1-interacting.
- **B. and C.** *IWS1 interacts with the SETD2 WW domain.* NCI-H522 and NCI-H1299 cells were transiently transfected with the indicated HA-SETD2 mutants. HA-SETD2 immunoprecipitates were probed with anti-IWS1 or Anti-HA (SETD2), antibodies. Input lysates were probed with anti-IWS1 and anti-Lamin A/C(NC-H522 cells) or anti-β-actin (NCI-H1299 cells) antibodies.

Figure 2

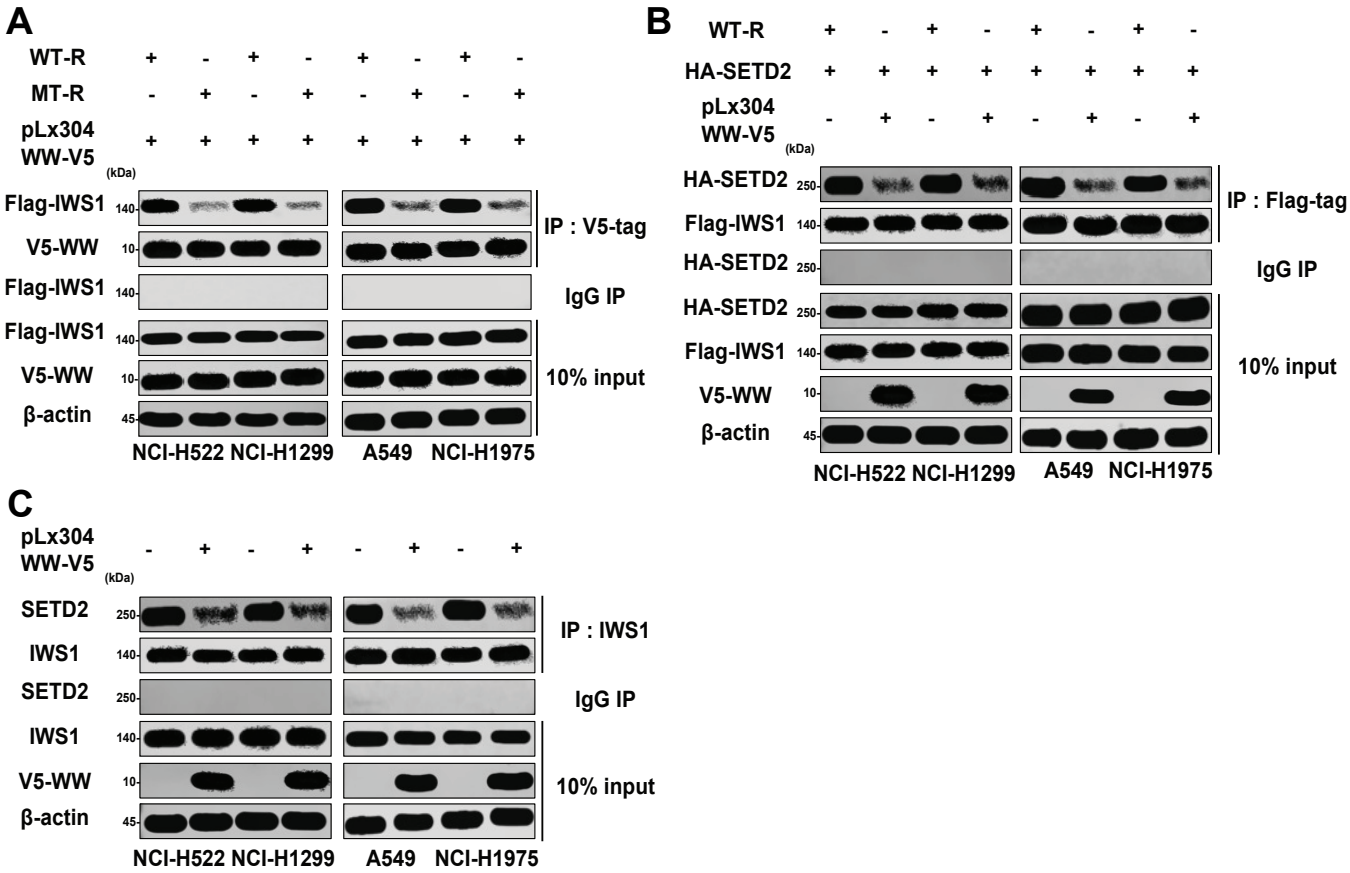
A
WT-R
MT-R
pLx304 WW-V5
(kDa)
Flag-IWS1
V5-WW
β-actin
IP : V5-tag
IgG IP
10% input
NCI-H522 NCI-H1299 A549 NCI-H1975
B
WT-R
HA-SETD2
pLx304 WW-V5
(kDa)
HA-SETD2
Flag-IWS1
V5-WW
β-actin
IP : Flag-tag
IgG IP
10% input
NCI-H522 NCI-H1299 A549 NCI-H1975
C
pLx304 WW-V5
(kDa)
SETD2
IWS1
V5-WW
β-actin
IP : IWS1
IgG IP
10% input
NCI-H522 NCI-H1299 A549 NCI-H1975

Figure 2. SETD2-WW domain binds selectively phosphorylated IWS1 and disrupts the interaction of endogenous IWS1 and SETD2

A. *The WW domain of SETD2 interacts selectively with phosphorylated exogenous IWS1 in multiple cell lines.* WT-R and MT-R NCI-H522, NCI-H1299 (Left panel), A549 and NCI-H1975 (Right panel) cells, were transduced with a SETD2 WW domain-V5 construct. Anti-V5 (WW domain) immunoprecipitates, were probed with anti-Flag (IWS1), or anti-V5 (WW domain), antibodies. IgG rabbit isotype control mock immunoprecipitates were probed with the anti-Flag (IWS1) antibody. Input lysates, were also probed with anti-Flag (IWS1), anti-V5 (WW domain), or anti-β-actin (loading control) antibodies.

B. *The WW domain of SETD2 interferes with the interaction of exogenous Flag-IWS1 and HA-SETD2 in multiple cell lines.* WT-R NCI-H522, NCI-H1299 (Left panel), A549 and NCI-H1975 cells (Right panel), were transduced with HA-SETD2 and HA-SETD2 WW domain constructs, as indicated. Anti-Flag (IWS1) immunoprecipitates and mock immunoprecipitates, as well as input lysates, were probed with anti-HA (SETD2), or anti-Flag (IWS1) antibodies. were probed with the anti-HA (SETD2) antibody. IgG rabbit isotype control mock immunoprecipitates were probed with anti-HA (SETD2) anti-Flag (IWS1), anti-V5 (WW domain) and β-actin (loading control) antibodies.

C. *The WW domain of SETD2 interferes with the interaction of endogenous IWS1 and SETD2 in multiple cell lines.* NCI -H522, NCI-H1299 (Left panel), A549 and NCI-H1975 cells (Right panel), were transduced with the V5-tagged construct of the WW domain of SETD2. Anti-IWS1 immunoprecipitates and IgG rabbit isotype control mock immunoprecipitates and input lysates were probed with the indicated antibodies.

Figure 3

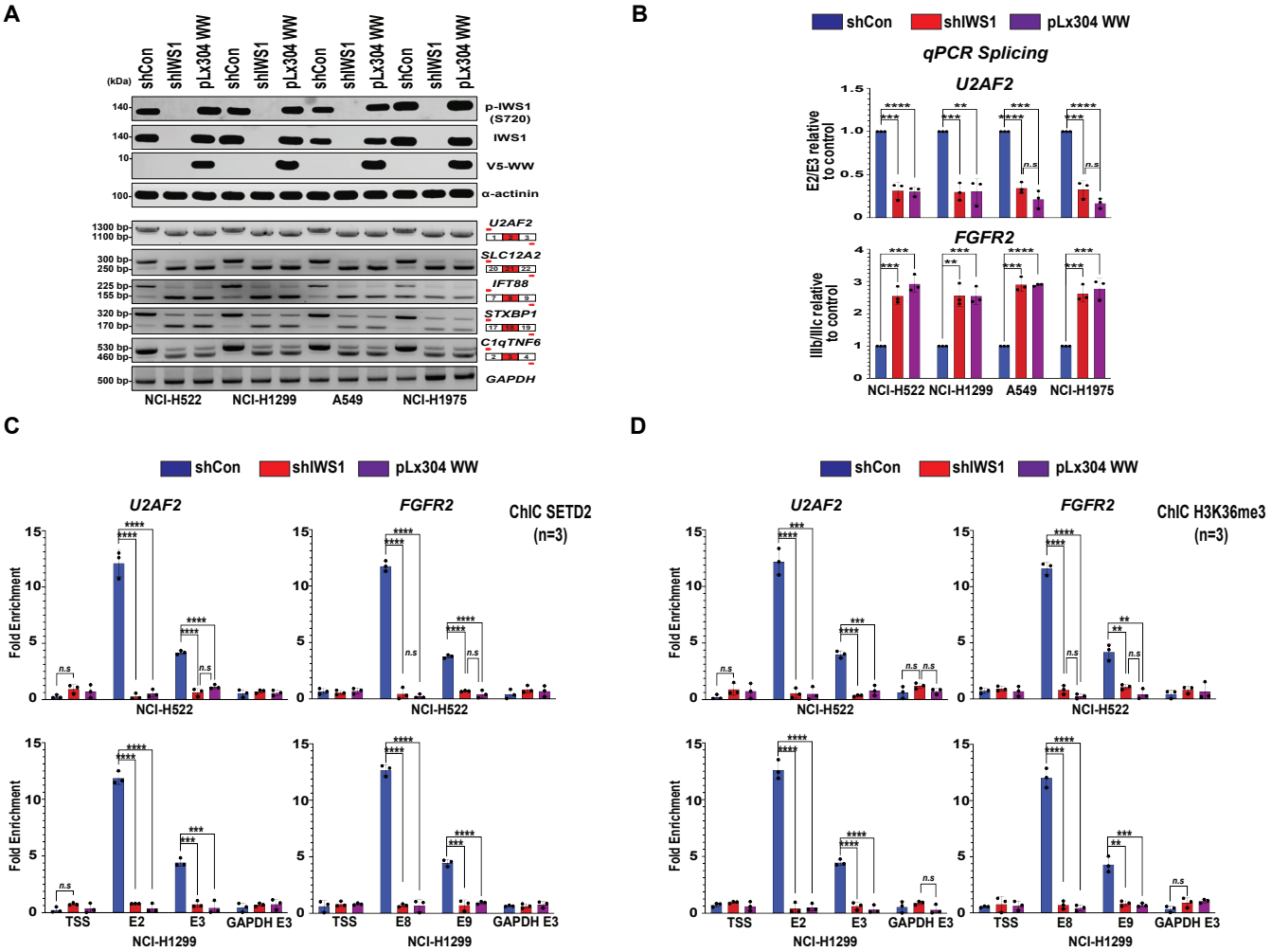
A
shCon
shIWS1
pLx304 WW
(kDa)
140
10
100
p-IWS1 (S720)
IWS1
V5-WW
α-actinin
1300 bp
1100 bp
300 bp
250 bp
225 bp
155 bp
320 bp
170 bp
530 bp
460 bp
500 bp
U2AF2
SLC12A2
IFT88
STXBP1
C1qTNF6
GAPDH
NCI-H522
NCI-H1299
A549
NCI-H1975
B
qPCR Splicing
U2AF2
E2/E3 relative to control
FGFR2
IIIb/IIIc relative to control
C
ChIC SETD2 (n=3)
Fold Enrichment
TSS
E2
E3
GAPDH E3
E8
E9
D
ChIC H3K36me3 (n=3)
n.s

Figure 3. The overexpression of SETD2 WW domain inhibits the IWS1 phosphorylation-dependent RNA splicing program.

A. *Overexpression of the WW domain of SETD2 inhibits the IWS1-dependent RNA splicing program.* (Upper rows) NCI-H522, NCI-H1299, A549 and NCI-H1975 cells were transduced with the SETD2 WW domain construct and their lysates were probed with antiphosphor-IWS1, anti-IWS1, anti-V5 (WW domain) and anti-α-actinin (Loading control) antibodies. Lysates of the same cell lines, transduced with the empty vector, or shIWS1, were harvested and probed with the same antibodies. (Lower rows) RT-PCR examining the exon usage of the known IWS1 RNA splicing targets *U2AF2* (exon 2), *SLC12A2* (exon 21), *IFT88* (exon 8), *STXBP1* (exon 18) and *C1qTNF6* (exon 3). *GAPDH* was used as control.

B. Quantitative RT-PCR showing the E2/E3 ratio of *U2AF2* (upper panel) and the IIIb/IIIc transcript ratio of *FGFR2* (lower panel) in shControl, shIWS1 and SETD2 WW-V5-transduced NCI-H522, NCI-H1299, A549 and NCI-H1975 cells. Bars show the *U2AF2* E2/E3 ratio or The FGFR2 IIIb/IIIc ratio (mean ± SD) relative to the shControl.

C. and D. ChIC assays addressing the binding of SETD2 and the abundance of H3K36me3 marks in the indicated regions of the *U2AF2*, *FGFR2* and *GAPDH* genes, in the NCI-H522 and NCI-H1299 cells shown in 3A. Bars show the mean fold enrichment (anti-SETD2 IP and anti-H3K36me3 IP vs IgG mock IP) ±SD. Data were normalized relative to the input (2%). All assays were done in triplicate, on three biological replicates. n.s : non-significant *$p<0.05$, **$p<0.01$, ***$p<0.001$, ****$p<0.0001$. (one-sided unpaired t-test)

Figure 4

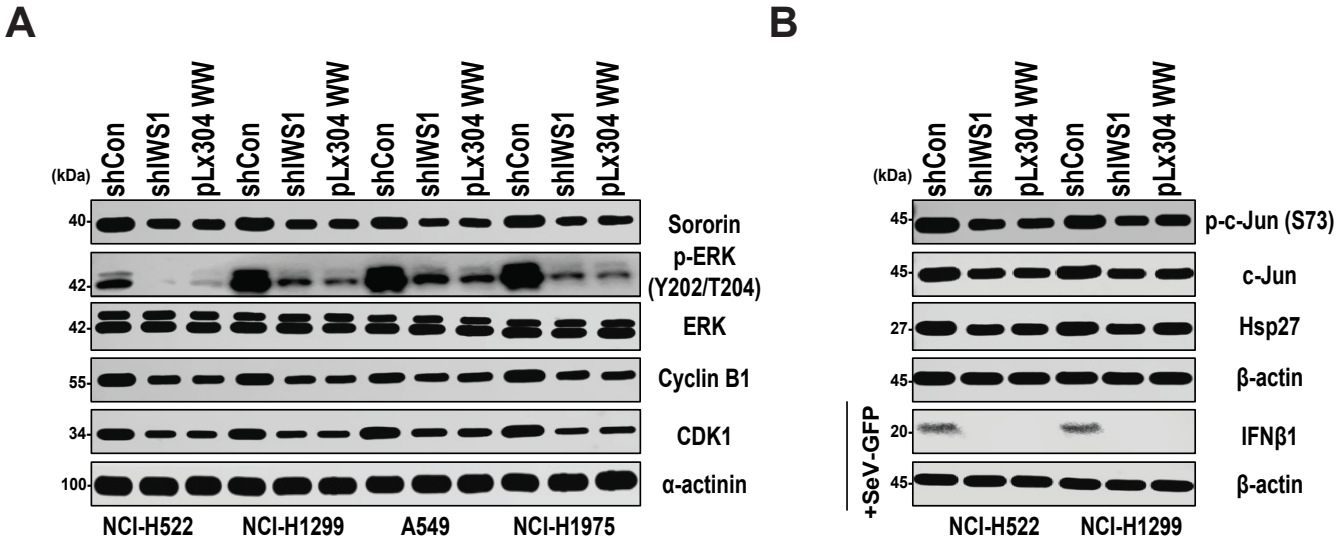
A
(kDa)
shCon
shIWS1
pLx304 WW
40-
42-
42-
55-
34-
100-
Sororin
p-ERK
(Y202/T204)
ERK
Cyclin B1
CDK1
α-actinin
NCI-H522
NCI-H1299
A549
NCI-H1975
B
(kDa)
shCon
shIWS1
pLx304 WW
45-
45-
27-
45-
20-
45-
p-c-Jun (S73)
c-Jun
Hsp27
β-actin
IFNβ1
β-actin
+SeV-GFP
NCI-H522
NCI-H1299

Figure 4. Overexpression of the SETD2 WW domain inhibits the IWS1 phosphorylation-dependent regulation of the cell cycle and the abundance of proteins encoded by CAR-E-positive intronless genes.

A. NCI-H522, NCI-H1299, A549 and NCI-H1975 cells, were transduced with the SETD2 WW domain construct. The same cells were transduced either with shIWS1 or empty vector (Control) constructs. Lysates of these cells were probed, with antibodies to cell cycle regulators, known to be under the control of the IWS1 phosphorylation pathway.

B. Lysates of NCI-H522 and NCI-H1299 cells transduced with the same constructs as the cells in a, were probed with antibodies specific to proteins encoded by CAR-E-positive intronless genes, or with an anti-β-actin antibody (loading control). Cells probed with antibodies to IFNβ1, were infected with a GFP-expressing Sendai virus (Sev-GFP) 16 hours prior to harvesting (MOI=0.5), or 24 hours prior to harvesting (MOI= 0.25), for NCI-H522 and NCI-H1299, respectively.

Figure 5

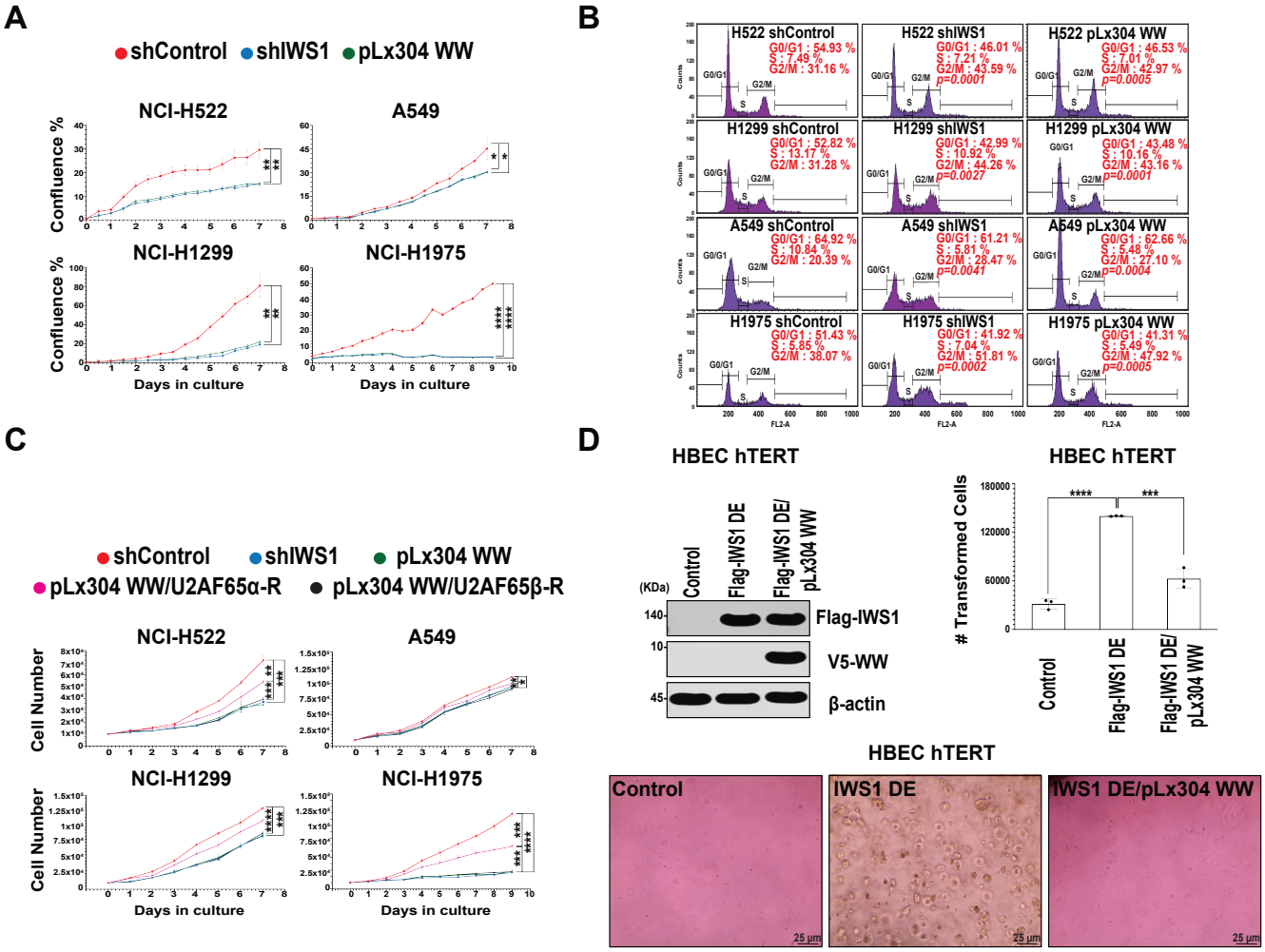
A
shControl
shIWS1
pLx304 WW
NCI-H522
A549
NCI-H1299
NCI-H1975
Confluence %
Days in culture
B
H522 shControl
G0/G1 : 54.93 %
S : 7.49 %
G2/M : 31.16 %
H522 shIWS1
G0/G1 : 46.01 %
S : 7.21 %
G2/M : 43.59 %
p=0.0001
H522 pLx304 WW
G0/G1 : 46.53 %
S : 7.01 %
G2/M : 42.97 %
p=0.0005
H1299 shControl
G0/G1 : 52.82 %
S : 13.17 %
G2/M : 31.28 %
H1299 shIWS1
G0/G1 : 42.99 %
S : 10.92 %
G2/M : 44.26 %
p=0.0027
H1299 pLx304 WW
G0/G1 : 43.48 %
S : 10.16 %
G2/M : 43.16 %
p=0.0001
A549 shControl
G0/G1 : 64.92 %
S : 10.84 %
G2/M : 20.39 %
A549 shIWS1
G0/G1 : 61.21 %
S : 5.81 %
G2/M : 28.47 %
p=0.0041
A549 pLx304 WW
G0/G1 : 62.66 %
S : 5.48 %
G2/M : 27.10 %
p=0.0004
H1975 shControl
G0/G1 : 51.43 %
S : 5.85 %
G2/M : 38.07 %
H1975 shIWS1
G0/G1 : 41.92 %
S : 7.04 %
G2/M : 51.81 %
p=0.0002
H1975 pLx304 WW
G0/G1 : 41.31 %
S : 5.49 %
G2/M : 47.92 %
p=0.0005
Counts
FL2-A
C
shControl
shIWS1
pLx304 WW
pLx304 WW/U2AF65α-R
pLx304 WW/U2AF65β-R
NCI-H522
A549
NCI-H1299
NCI-H1975
Cell Number
Days in culture
D
HBEC hTERT
(KDa)
Control
Flag-IWS1 DE
Flag-IWS1 DE/ pLx304 WW
140
10
45
Flag-IWS1
V5-WW
β-actin
Transformed Cells
Control
IWS1 DE
IWS1 DE/pLx304 WW
25 µm

Figure 5. The overexpression of SETD2 WW domain induces partial G2/M arrest in lung adenocarcinoma cell lines and anchorage-independent growth in hTert-immortalized human bronchial epithelial cells (hTert HBEC).

A. *Growth curves of NCI-H522, NCI-H1299, A549 and NCI-H1975 cells transduced with the SETD2 WW domain construct.* The same cells, transduced with the shIWS1 construct or the empty vector were used as controls. Cells were grown under normal growth conditions in complete media supplemented with 10% FBS. Cell proliferation was monitored at 6 hour intervals by "Incucyte" imaging. Data are presented as the mean percentage of confluence ±SD. For simplicity, only 12h time-points are shown. *P* values of the difference were calculated for the last measurements for each cell line, using the one-sided unpaired t-test. *p<0.05, **p<0.01, ***p<0.001, ****p<0.0001

B. *Cell cycle profiles of the cell lines shown in a.* Propidium iodide (PI)-stained cells were analyzed by flow-cytometry to determine their distribution in different phases of the cell cycle. Experiments were done on three biological replicates. Numbers in red show the mean percentage of cells in different phases of the cell cycle and *P* values of the differences between shControl and shIWS1 or shControl and pLx304 WW-transduced cells, were calculated using the unpaired one-sided t test.

C. Growth curves of NCI-H522, NCI-H1299, A549 and NCI-H1975 cells transduced with shControl, shIWS1, or pLX304-WW domain constructs were rescued with U2AF65α, or U2AF65β, were grown in media supplemented with 10% FBS. Live-cell numbers (mean ±SD) were measured with the alamarBlue™ Cell Viability Reagent in three independent cultures for each cell type. The expression of V5-U2AF65 splice variants is shown in Supplementary Figure 1A.

D. *Overexpression of the WW domain of SETD2 inhibits the anchorage-independent growth of hTert-HBECs, transformed by IWS1 S720D/T721E (IWS1 DE).* (Upper left panel). Expression of Flag-IWS1 DE and V5-WW domain in hTert HBECs, transduced with the corresponding constructs. Cell lysates were probed with anti-Flag (IWS1), anti-

V5 (WW domain) or anti-β-actin (loading control) antibodies. (Lower panel) Cells in the upper left panel were cultured in soft agar and they were imaged 7 days later. Scale bar is shown on the right lower corner of each image. (Upper right panel) After imaging, the cells were incubated in WST solution (Cell Transformation Assay Kit-Abcam) for 4 hours. Bars show the relative number of cells growing in soft agar ±SD. The number was calculated from the absorbance at 450 nm. All assays were done in triplicate, on three biological replicates. n.s: non-significant *$p<0.05$, **$p<0.01$, ***$p<0.001$, ****$p<0.0001$. (one-sided unpaired t-test).

Figure 6

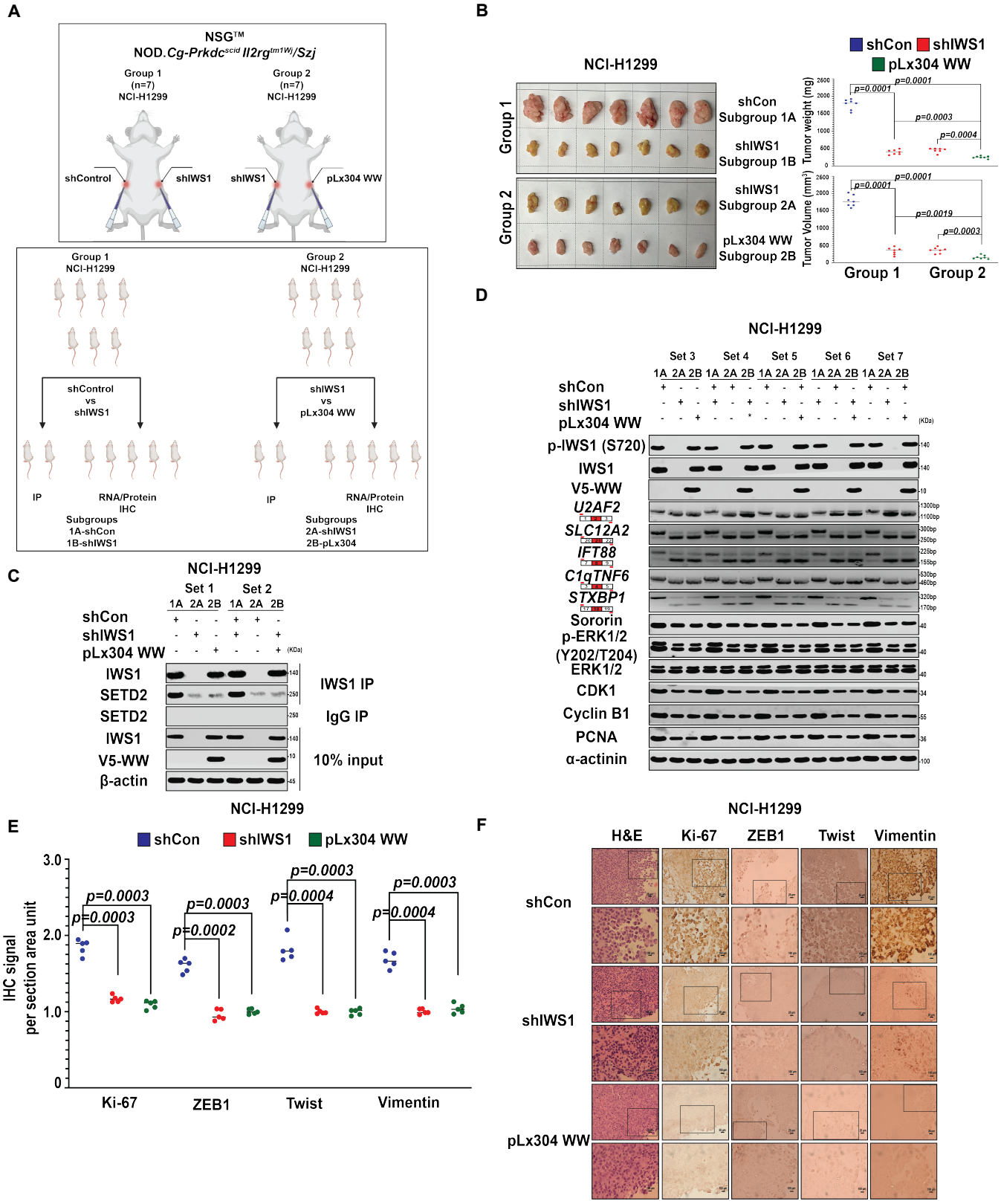
A
NSG™
NOD.Cg-Prkdc^scid Il2rg^tm1Wj/Szj
Group 1 (n=7) NCI-H1299
Group 2 (n=7) NCI-H1299
shControl
shIWS1
shIWS1
pLx304 WW
Group 1 NCI-H1299
Group 2 NCI-H1299
shControl vs shIWS1
shIWS1 vs pLx304 WW
IP
RNA/Protein IHC
Subgroups 1A-shCon 1B-shIWS1
IP
RNA/Protein IHC
Subgroups 2A-shIWS1 2B-pLx304
B
NCI-H1299
shCon
shIWS1
pLx304 WW
Group 1
Group 2
shCon Subgroup 1A
shIWS1 Subgroup 1B
shIWS1 Subgroup 2A
pLx304 WW Subgroup 2B
Tumor weight (mg)
Tumor Volume (mm³)
p=0.0001
p=0.0003
p=0.0004
p=0.0019
Group 1
Group 2
C
NCI-H1299
Set 1
Set 2
shCon
shIWS1
pLx304 WW
IWS1
SETD2
SETD2
IWS1
V5-WW
β-actin
IWS1 IP
IgG IP
10% input
D
NCI-H1299
Set 3
Set 4
Set 5
Set 6
Set 7
shCon
shIWS1
pLx304 WW
p-IWS1 (S720)
IWS1
V5-WW
U2AF2
SLC12A2
IFT88
C1qTNF6
STXBP1
Sororin
p-ERK1/2 (Y202/T204)
ERK1/2
CDK1
Cyclin B1
PCNA
α-actinin
E
NCI-H1299
shCon
shIWS1
pLx304 WW
IHC signal per section area unit
p=0.0003
p=0.0003
p=0.0003
p=0.0002
p=0.0003
p=0.0004
p=0.0003
p=0.0004
Ki-67
ZEB1
Twist
Vimentin
F
NCI-H1299
H&E
Ki-67
ZEB1
Twist
Vimentin
shCon
shIWS1
pLx304 WW

Figure 6. Overexpression of the WW domain of SETD2 in the lung adenocarcinoma cell line NCI-H1299 inhibits the IWS1 phosphorylation pathway and tumor growth and *in vivo*.

A. *Summary of the experimental design.* (Upper panel) Two groups of 7 NSG mice were inoculated SC with $2x10^6$ NCI-H1299 cells, as shown. Group 1 compared the in vivo growth of shControl (subgroups 1A and 1B) and shIWS1 cells and group 2 compared the in vivo growth of shIWS1-transduced and pLX304 WW domain-transduced cells (subgroups 2A and 2B). (Lower panel) IWS1 was immunoprecipitated from lysates of the tumors developing in two mice in each group and the immunoprecipitates were probed with the anti-SETD2 antibody to determine whether IWS1 and SETD2 interact. The tumors developing in the remaining five mice in each group were used for RT-PCR and western blotting. Histology and immunohistochemistry experiments were carried out on 5 randomly picked tumors from each subgroup.

B. Tumors developing in mice of both groups were harvested at 4 weeks from the time of inoculation. (Left panel) Pictures of all the harvested tumors. (Right panel) Weight and volume of the same tumors. The horizontal lines indicate mean tumor weight or volume. Statistical analyses were done using the one-sided paired t-test.

C. *Overexpression of the WW domain of SETD2 inhibits the IWS1/SETD2 interaction in tumor xenografts.* IWS1 was immunoprecipitated from lysates of two tumor xenografts from each subgroup. The anti-IWS1 immunoprecipitates were probed with anti-IWS1 or anti-SETD2 antibodies. IgG mock immunoprecipitates were probed with the anti-SETD2 antibody. Input lysates were probed with anti-IWS1, anti-V5 (WW domain), or anti-β-actin antibodies

D. *Overexpression of the WW domain of SETD2 inhibits IWS1 phosphorylation-dependent alternative RNA splicing and U2AF2 RNA splicing-dependent expression and modification of regulators of the cell cycle.* RT-PCR of *U2AF2* E2, *SLC12A2* E21,

IFT88 E8, *C1qTNF6* E3, *STXBP1* E18, using RNA derived from the mouse xenografts in a. Lysates from the same xenografts were probed with the indicated antibodies.

E. Formalin-fixed, paraffin-embedded tumor samples were stained with the indicated antibodies. Secondary antibody was HRP-labelled. Scatter plots of the IHC signals obtained from representative equal size areas of the indicated xenografts. The horizontal lines show the mean signal for each group of xenografts. Statistical analyses were performed, using the one-sided paired t-test.

F. Representative IHC images of tumor xenografts. Scale in the right lower corner of each image.

Figure 7

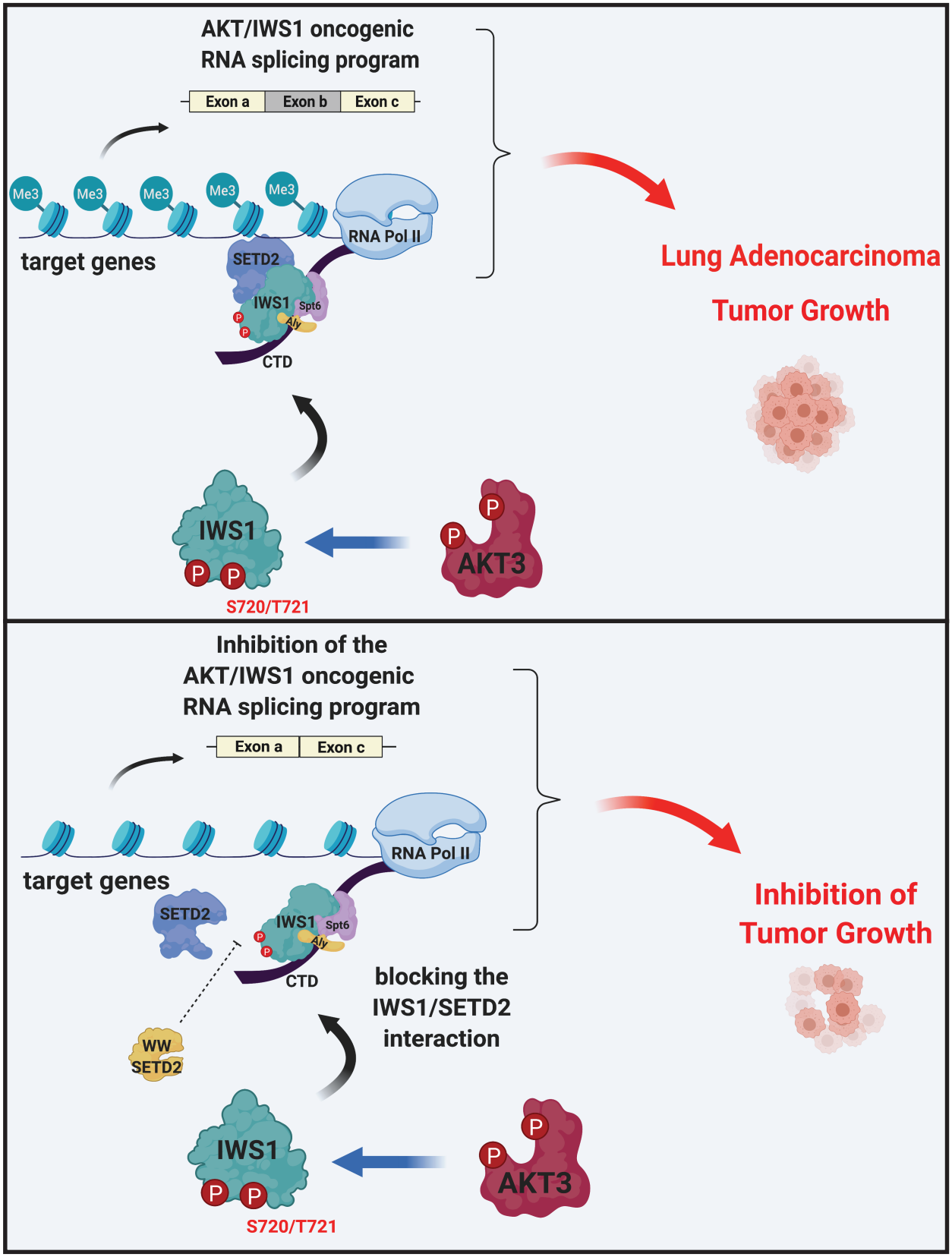
AKT/IWS1 oncogenic
RNA splicing program
Exon a
Exon b
Exon c
Me3
target genes
SETD2
RNA Pol II
IWS1
Spt6
Aly
CTD
Lung Adenocarcinoma
Tumor Growth
IWS1
P
S720/T721
AKT3
Inhibition of the
AKT/IWS1 oncogenic
RNA splicing program
Exon a
Exon c
target genes
RNA Pol II
SETD2
IWS1
Spt6
Aly
CTD
blocking the
IWS1/SETD2
interaction
WW
SETD2
Inhibition of
Tumor Growth
IWS1
S720/T721
AKT3

Figure 7. Graphical abstract of the findings.

Overexpression of the SETD2 WW domain antagonizes the interaction of SETD2 with phosphorylated IWS1 and the recruitment of SETD2 to the SPT6/IWS1 complex, assembling on the Ser2-phosphorylated CTD of RNA Pol II. Interference with the recruitment of SETD2 prevents histone H3K36 trimethylation and subsequent H3K36me3-dependent RNA processing. The ultimate outcome of the WW domain-dependent inhibition of the recruitment of SETD2 to the SPT6/phosphor-IWS1 complex is the inhibition of tumor growth.